Inhibition of Cell Migration, Spreading, and Focal Adhesions by Tumor Suppressor PTEN

Masahito Tamura,* Jianguo Gu, Kazue Matsumoto, Shin-ichi Aota, Ramon Parsons, Kenneth M. Yamada*

The tumor suppressor PTEN is a phosphatase with sequence similarity to the cytoskeletal protein tensin. Here the cellular roles of PTEN were investigated. Overexpression of PTEN inhibited cell migration, whereas antisense PTEN enhanced migration. Integrin-mediated cell spreading and the formation of focal adhesions were down-regulated by wild-type PTEN but not by PTEN with an inactive phosphatase domain. PTEN interacted with the focal adhesion kinase FAK and reduced its tyrosine phosphorylation. Overexpression of FAK partially antagonized the effects of PTEN. Thus, PTEN phosphatase may function as a tumor suppressor by negatively regulating cell interactions with the extracellular matrix.

The gene *PTEN* (also called MMAC1) is a tumor suppressor gene on human chromosome 10q23 that is frequently deleted or mutated in ~45% of endometrial cancers, ~30% of glioblastomas, and at lesser frequencies in a wide range of other human tumors (*1*, *2*). *PTEN* encodes the catalytic signature motif of protein tyrosine phosphatases and functions as a dual-specificity phosphatase in vitro (*3*, *4*). Expression of *PTEN* cDNA in glioma cells with mutated *PTEN* alleles suppresses growth, but it does not affect the growth of cells with wild-type *PTEN* alleles (*5*). The physiological substrates and functions of PTEN protein, however, remain to be elucidated. PTEN also has sequence similarity to tensin (*1*), a cytoskeletal protein that binds to actin filaments at focal adhesions and is tyrosine phosphorylated upon integrin-mediated cell adhesion (*6*). PTEN might therefore have effects on integrin function or on the cytoskeleton.

We investigated whether PTEN participates in cell migration, growth, spreading, and cytoskeletal regulation through transfection experiments with four cell types. Stable transfectant lines of NIH 3T3 fibroblasts were established in which the expression of *PTEN* was regulated by ecdysone, using expression plasmids containing sense *PTEN*, antisense *PTEN*, or no insert (*7*). A twofold overexpression of PTEN mRNA significantly reduced cell migration as measured by in vitro wound healing assays (Fig. 1). In contrast, the expression of antisense *PTEN* enhanced cell migration (Fig. 1). Antisense-expressing cells migrated much farther (200 ± 92 cells/mm^2 migrated more than 0.4 mm from the wound edge in 24 hours) than mock- (7 ± 3 cells/mm^2) or sense-transfected cells (0 ± 0 cells/mm^2) (Fig. 1A). The number of migrating *PTEN*-overexpressing cells was decreased to 48% of mock (967 ± 138 compared with 2013 ± 63 cells/mm^2; $P < 0.001$), whereas the number of migrating antisense-expressing cells increased by 21% over mock (2440 ± 243 cells/mm^2; $P < 0.01$). With regard to cell growth, in contrast, expression of sense or antisense *PTEN* had little effect (*8*), consistent with a previous report (*5*).

To explore the mechanism underlying the effect of PTEN on NIH 3T3 cell migration, we examined cell spreading on fibronectin (FN) (*9*). Although cell attachment appeared unaffected, stable transfectants induced by ecdysone to express sense *PTEN* showed a marked reduction in cell spreading. In a 30-min assay, only 20 ± 5% of these cells had spread, whereas 59 ± 6% of mock-transfected and 59 ± 6% of antisense *PTEN*–expressing cells had spread ($P < 0.001$) (Fig. 2A). Similar results were obtained with two other independent sets of ecdysone-regulated transfectants.

The role of PTEN in cell spreading was also examined in transiently transfected primary human fibroblasts and DBTRG-05MG cells, a glioblastoma cell line with a 204–base pair deletion in *PTEN* (*1*). Cells expressing the various constructs were detected by using green fluorescent protein (GFP) as a marker (*10*). Again, PTEN inhibited cell spreading on FN (Fig. 2, B and C). In human fibroblasts, the effect was maximal at 20 to 30 min, with only 22 ± 8% of *PTEN*-overexpressing cells spread at 30 min compared with 60 ± 8% of nontransfected cells or cells with control GFP-plasmid ($P < 0.001$ to 0.005) (Fig. 2C). The majority of cells had spread by 2 hours, however, indicating that *PTEN* overexpression delayed but did not prevent spreading. Nevertheless, the surface area covered by *PTEN*-expressing cells remained less than that of controls (see below). In DBTRG-05MG cells, exogenous expression of *PTEN* also delayed spreading; even after 18 hours, only 64% of the cells had spread, and the extent of spreading of individual cells was substantially reduced (Fig. 2B). Inhibition of spreading was also observed in *PTEN*-transfected U-87MG cells, a glioblastoma

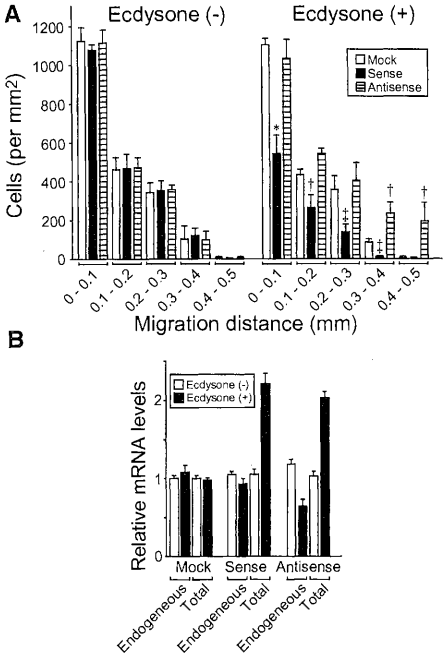

Fig. 1. PTEN modulation of cell migration. Stable NIH 3T3 cell transfectants were induced to express *PTEN* or antisense *PTEN* in an ecdysone expression system (*7*). (**A**) In vitro "scratch" wounds were created by scraping confluent cell monolayers in fibronectin-coated (10 μg/ml) petri dishes (35-mm diameter) with a sterile pipette tip. After 24 hours, migration was quantified by counting cell numbers at the indicated migration distances from the wound edge. Error bars indicate standard deviation; *, $P < 0.005$; †, $P < 0.01$; ‡, $P < 0.05$, respectively (versus mock) by Student's *t* test. (**B**) Levels of endogenous, antisense, or total PTEN mRNA were determined by quantitative reverse transcription–polymerase chain reaction (RT-PCR; primer sequences provided on request). Preliminary protein immunoblot analysis showed roughly similar changes in PTEN protein expression (*8*).

M. Tamura, J. Gu, K. Matsumoto, S. Aota, K. M. Yamada, Craniofacial Developmental Biology and Regeneration Branch, National Institute of Dental Research, National Institutes of Health, Building 30, Room 421, 30 Convent Drive MSC 4370, Bethesda, MD 20892–4370, USA.
R. Parsons, Departments of Pathology and Medicine, College of Physicians and Surgeons, Columbia University, 630 West 168th Street, New York, NY 10032, USA.
*To whom correspondence should be addressed. E-mail: mtamura@yoda.nidr.nih.gov or kyamada@yoda.nidr.nih.gov

line with a *PTEN* frameshift mutation at codon 54 (see Fig. 5B, which will be fully discussed below).

Down-modulation of cell spreading by PTEN could have resulted from effects on integrin-mediated cell spreading or on cytoskeletal processes required for cell spreading. To distinguish between these possibilities, we compared the effects of *PTEN* overexpression on cell interactions with integrin versus nonintegrin ligands. Cell spreading occurred normally on nonintegrin substrates of polylysine and concanavalin A even with *PTEN* overexpression, indicating that there was no defect in the intracellular machinery involved in cell spreading (Fig. 2D). In contrast, cells on all integrin-interacting substrates tested [FN, vitronectin, and a monoclonal antibody (mAb) to β_1 integrin (*11*)] showed substantial inhibition of spreading at the 30-min time point. Thus, *PTEN* overexpression appears to reduce integrin-mediated cell spreading selectively.

We next examined the effect of PTEN on focal adhesion formation (*12*). After 2 hours of adhesion to FN, human foreskin fibroblasts transfected with control or antisense *PTEN* plasmids formed numerous focal adhesions, which contained paxillin, vinculin, focal adhesion kinase (FAK), and localized phosphotyrosine (Fig. 3, A and B, arrowheads). In *PTEN*-transfected cells (detected by GFP fluorescence), the total number of focal adhesions was substantially reduced in comparison with controls (Fig. 3, A and B). However, staining intensities were similar for each of these components [and tensin (*8*)] within the remaining focal adhesions. *PTEN* also down-regulated actin microfilament (stress fiber) formation as determined by staining with rhodamine-labeled phalloidin (Fig. 3A).

In U-87MG cells, *PTEN* also altered cell morphology and down-regulated actin microfilament formation. Phosphatase-inactivating mutations in *PTEN* (*13*) destroyed its ability to induce cytoskeletal and morphological effects (Fig. 3C). In contrast, the *PTEN* mutant G129E that retains phosphatase activity (*3*) behaved like wild-type *PTEN* in these assays (Fig. 3C). Moreover, cells

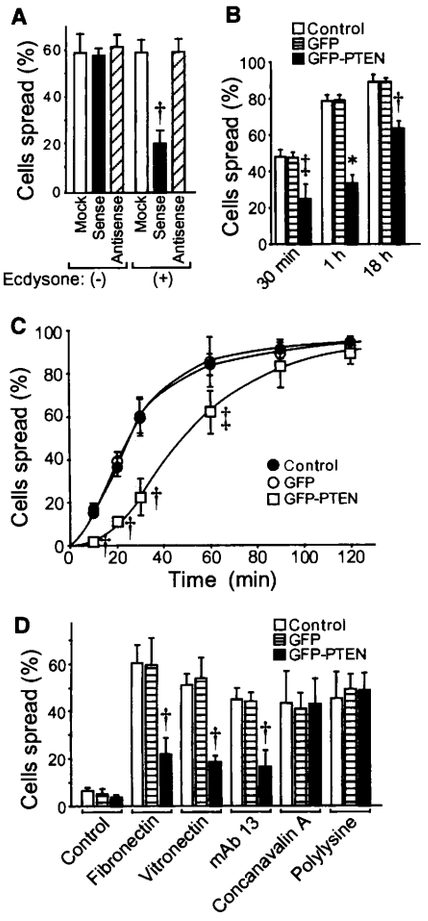

Fig. 2. PTEN inhibition of cell spreading. (**A**) NIH 3T3 cell transfectants expressing sense or antisense *PTEN* induced by ecdysone were allowed to spread on cover slips coated with FN (10 μg/ml) and then fixed with 4% paraformaldehyde. The percentage of cells spread on FN was determined. (**B**) Spreading of DBTRG-05MG cells on FN after transient transfection with GFP as a marker for transfection or with GFP-*PTEN*; $n = 3$ experiments. (**C**) Spreading of human foreskin fibroblasts on FN. Black circles, nontransfected control; white circles, GFP transfected; squares, GFP-*PTEN* transfected ($n = 3$ to 5 experiments). (**D**) Human foreskin fibroblasts were plated on cover slips that were uncoated or coated with FN (10 μg/ml), vitronectin (25 μg/ml), mAb 13 (50 μg/ml; an antibody to β_1 integrin), concanavalin A (25 μg/ml), or polylysine (25 μg/ml). The percentage of cells spread after 30 min was determined; $n = 3$ experiments. Error bars indicate standard deviation; *, $P < 0.0005$; †, $P < 0.001$; ‡, $P < 0.005$, respectively, versus control.

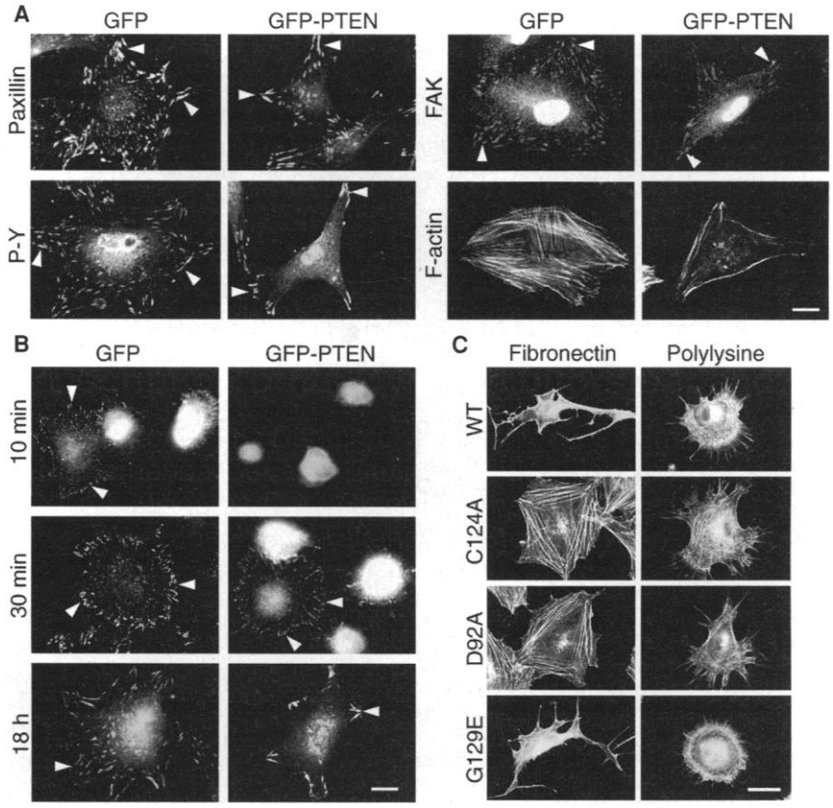

Fig. 3. PTEN modulation of focal adhesion formation. (**A**) Human foreskin fibroblasts transfected with GFP or GFP-*PTEN* were allowed to spread on FN-coated cover slips for 2 hours and were then immunostained with antibodies to paxillin, phosphotyrosine (P-Y), or FAK, or stained with rhodamine-phalloidin to detect F-actin. Arrowheads indicate focal adhesions. (**B**) Human fibroblasts expressing GFP or GFP-*PTEN* were stained with antibody to vinculin (anti-vinculin) 10 min, 30 min, or 18 hours after plating on FN-coated cover slips. Arrowheads indicate focal adhesions. (**C**) U-87MG cells transfected with GFP-tagged wild type (WT) *PTEN* or the indicated *PTEN* mutants (*13*) were allowed to spread on FN- or polylysine-coated cover slips for 2 hours and stained with rhodamine-phalloidin. Scale bars, 10 μm.

transfected by all *PTEN* mutants spread similarly on the nonspecific adhesive substrate polylysine (Fig. 3C), confirming the integrin dependence of the *PTEN* effects. In DBTRG-05MG cells, focal adhesion formation was also suppressed in *PTEN*-expressing cells even after an 18-hour incubation on FN (*8*). Thus, PTEN can down-modulate integrin-mediated focal adhesion formation and organization of the actin-containing cytoskeleton in a phosphatase-dependent manner. In contrast, human foreskin fibroblasts and U-87MG cells overexpressing another nonreceptor protein tyrosine phosphatase, PTP1B, showed no detectable change in cell spreading and cytoskeletal formation (*8*), consistent with a previous study (*14*).

Cell interactions with extracellular matrix proteins through integrin receptors can mediate transmembrane signal transduction, including integrin-mediated tyrosine phosphorylation of FAK (*15*). PTEN suppressed tyrosine phosphorylation of FAK after adhesion to FN (Fig. 4A). Two clones of *PTEN*-overexpressing NIH 3T3 cells showed >60% decreases in tyrosine phosphorylation of FAK 2 hours after plating on FN (38 ± 7% of controls in five experiments, $P < 0.001$). This effect persisted for more than 18 hours after plating on FN (*8*), accompanied by decreased numbers of focal adhesions (Fig. 3B). The effects appeared to be relatively selective for FAK phosphorylation, because phosphotyrosine staining of many other proteins was unchanged (Fig. 4A). Immunoprecipitation of individual phosphoproteins showed similar decreases in tyrosine phosphorylation of FAK and the putative downstream target $p130^{Cas}$, but not in phosphorylation of paxillin, c-Src, or tensin (Fig. 4B). Whether $p130^{Cas}$ is a direct or indirect substrate for PTEN remains to be determined. In experiments with U-87MG cells, inhibition of FAK phosphorylation (Fig. 5A) and cell spreading (Fig. 5B) occurred only when the cells were transfected with phosphatase-active forms of PTEN. The relatively selective dephosphorylation of FAK and $p130^{Cas}$ by PTEN may be particularly relevant to cell migration. Both FAK and $p130^{Cas}$ have been implicated directly in up-regulating cell migration through tyrosine phosphorylation of each molecule (*16*)

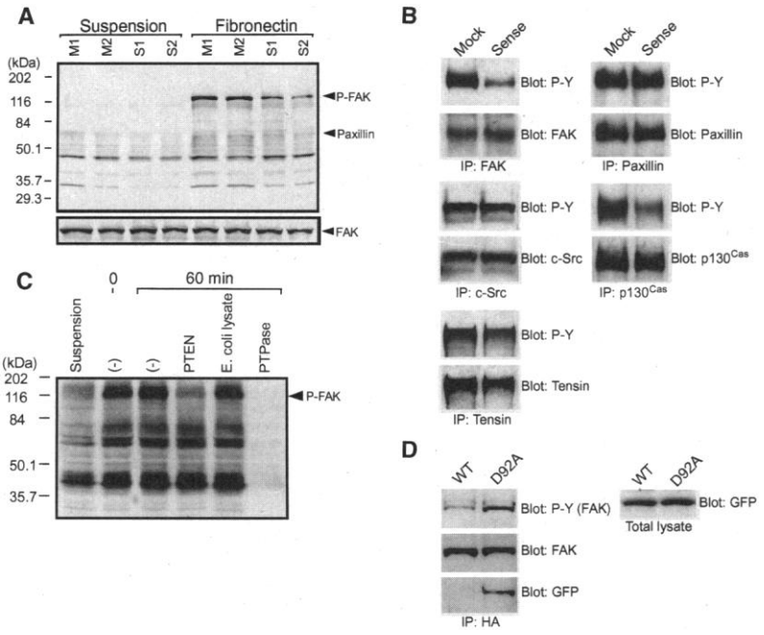

Fig. 4. (**A**) Inhibition of FAK tyrosine phosphorylation by PTEN. NIH 3T3 cells transfected with control plasmid lacking an insert (M1, M2) or with sense *PTEN* (S1, S2) were induced for 5 days with ecdysone, and lysates were prepared from cells in suspension or from cells allowed to spread on FN for 2 hours. Tyrosine phosphorylation was assessed by immunoblotting with anti-phosphotyrosine (*13*). The amount of FAK protein in each sample was assessed by immunoblotting a parallel gel (bottom panel) with anti-FAK. P-FAK, phosphorylated FAK. (**B**) Immunoprecipitation (IP) from NIH 3T3 transfectants of FAK, paxillin, c-Src, $p130^{Cas}$, and tensin followed by immunoblotting with anti-phosphotyrosine (P-Y) (*21*). (**C**) Direct tyrosine dephosphorylation of FAK by PTEN. After SDS-PAGE of U-87MG cell lysates, nitrocellulose blots were incubated with or without His-tagged recombinant PTEN (20 μg/ml), control *E. coli* lysate (200 μg/ml), or a 34-kD fragment of a recombinant protein tyrosine phosphatase (Boehringer Mannheim; 25 mU/ml, ~1 μg/ml). Tyrosine phosphorylation was visualized as in (A). (**D**) NIH 3T3 cells transfected with tracer levels of HA-FAK plus GFP-tagged wild-type *PTEN* or trapping mutant D92A were immunoprecipitated with anti-HA and immunoblotted for phosphotyrosine (P-Y), FAK, or GFP; the original lysate was immunoblotted for GFP to confirm similar amounts of GFP.

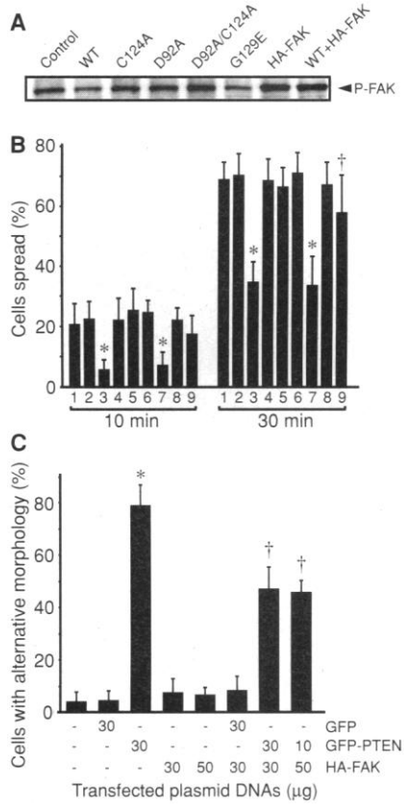

Fig. 5. Phosphatase-dependent inhibition of FAK tyrosine phosphorylation by PTEN and rescue by FAK coexpression. (**A**) U-87MG cells were transfected with 30 μg each of the indicated constructs (*13*) (control was mock transfected), and cell lysates were prepared from cells allowed to spread on FN for 2 hours. Tyrosine phosphorylation was assessed by immunoblotting with anti-phosphotyrosine. (**B**) Effects of PTEN mutants and FAK expression on cell spreading. U-87MG cells transfected with 30 μg of each construct were plated on FN-coated cover slips (*13*). The percentage of cells spread after 10 and 30 min was determined by double-blind scoring. 1, nontransfected cells; 2, GFP; 3 through 7, GFP-tagged PTEN (3, wild type; 4, C124A; 5, D92A; 6, D92A/C124A; 7, G129E control); 8, GFP + HA-FAK; and 9, wild-type GFP-PTEN + HA-FAK. *, $P < 0.0001$ versus control (lane 1); †, $P < 0.05$ versus wild-type PTEN (lane 3); and $P = 0.06$ versus control (lane 1). (**C**) Partial rescue by FAK coexpression of PTEN-induced morphology changes. U-87MG cells transfected with GFP, GFP-PTEN, and HA-FAK were plated on FN-coated cover slips for 2 hours. The percentage of cells with alternative morphology was determined by double-blind scoring. *, $P < 0.0001$ versus nontransfected cells; †, $P < 0.0001$ versus nontransfected cells (lane 1) or GFP-PTEN (lane 3).

We next tested whether PTEN could directly dephosphorylate tyrosine-phosphorylated FAK in vitro using an in-blot phosphatase assay (*17*). Total tyrosine-phosphorylated proteins from U-87MG cells were electroblotted and incubated with or without bacterially expressed PTEN, or with whole *Escherichia coli* lysate as a control for tyrosine phosphatase contamination (Fig. 4C). Recombinant PTEN reduced tyrosine phosphorylation of FAK by 64% (36.2 ± 9.9% of controls, four experiments, $P < 0.001$), with minimal effects on other phosphorylated protein bands in the blot. No dephosphorylation occurred without PTEN, and substitution of a broad-specificity tyrosine phosphatase removed phosphotyrosine from all bands (Fig. 4C). We emphasize that these data indicate a relative sensitivity of FAK to PTEN dephosphorylation compared with other phosphoproteins visible in these blots, not necessarily that FAK is its sole substrate.

We tested for physical interactions of PTEN with FAK in living cells using a "trapping" mutant (*18*) of PTEN. Overexpression of a PTEN mutant with inactivated phosphatase activity (potentially able to bind and protect a substrate) resulted in elevated phosphorylation of tracer levels of hemagglutinin (HA)–tagged FAK in NIH 3T3 cells (Fig. 4D). Moreover, immunoprecipitated HA-FAK retained bound GFP-PTEN, indicating formation of a FAK-PTEN complex (Fig. 4D). To investigate whether manipulating the amounts of phosphorylated FAK could antagonize the biological effects of PTEN, we overexpressed HA-tagged FAK with or without GFP-PTEN or GFP in U-87MG cells and assessed FAK phosphorylation and cell morphology. Overexpression of FAK abrogated PTEN-induced down-regulation of FAK phosphorylation (Fig. 5A) without decreasing amounts of GFP-PTEN. Although FAK overexpression alone had no effect on cell spreading (Fig. 5B) or on morphology and the actin cytoskeleton (Fig. 5C), coexpression of FAK with PTEN partially rescued the ability of cells to spread at normal rates (Fig. 5B), consistent with its role in cell spreading (*19*), and it reduced by 40% the number of cells with altered morphology and impaired cytoskeletal formation (Fig. 5C). We speculate that increasing FAK may enhance its phosphorylation either by increasing the total amount of FAK available for phosphorylation or by increasing integrin engagement during FAK-enhanced spreading. Regardless of its mechanism of action, FAK appears to be a target and effector of PTEN action.

Exogenous PTEN can suppress the growth of cells with mutated *PTEN* alleles (*5*), but our data also indicate that this tumor suppressor has cell biological activities unrelated to growth. In contrast to many other tumor suppressors, which appear to have only nuclear roles, PTEN also appears to function in regulating dynamic cell surface interactions that involve integrins, FAK, cell migration, and the cytoskeleton.

REFERENCES AND NOTES

1. J. Li *et al.*, *Science* **275**, 1943 (1997); P. A. Steck *et al.*, *Nature Genet.* **15**, 356 (1997).
2. D. Kong *et al.*, *Nature Genet.* **17**, 143 (1997); P. Guldberg *et al.*, *Cancer Res.* **57**, 3660 (1997); S. I. Wang *et al.*, *ibid.*, p. 4183; D. H. F. Teng *et al.*, *ibid.*, p. 5221; K. Okami *et al.*, *ibid.* **58**, 509 (1998).
3. M. P. Myers *et al.*, *Proc. Natl. Acad. Sci. U.S.A.* **94**, 9052 (1997).
4. D. M. Li and H. Sun, *Cancer Res.* **57**, 2124 (1997); L. Li, B. R. Ernsting, M. J. Wishart, D. L. Lohse, J. E. Dixon, *J. Biol. Chem.* **272**, 29403 (1997).
5. F. B. Furnari, H. Lin, H.-J. S. Huang, W. K. Cavenee, *Proc. Natl. Acad. Sci. U.S.A.* **94**, 12479 (1997).
6. S. Lin, in *Guidebook to the Cytoskeletal and Motor Proteins*, T. Kreis and R. Vale, Eds. (Oxford Univ. Press, Oxford, 1993), pp. 240–242.
7. Five sets each of stable NIH 3T3 cell transfectants were established with an ecdysone expression system based on pINDSP1 and pVgRXR (Invitrogen, Carlsbad, CA) with plasmids containing no insert, full-length human 5′ Flag epitope–tagged sense *PTEN*, or full-length antisense *PTEN* sequences. Expression was induced with 1 μM muristerone A for 5 days.
8. M. Tamura, J. Gu, K. M. Yamada, unpublished data.
9. Cell spreading was quantified as described previously (*11*, *20*) by scoring at least 100 cells per transfection and pooling data from three to five experiments.
10. GFP expression plasmid pGZ21δxZ was constructed by inserting GFP with a Kozak consensus sequence in a cytomegalovirus promoter-based expression system. Plasmid pGZ21δxZ (30 μg) containing either no insert or full-length *PTEN* was transfected into 1.5×10^6 human foreskin fibroblasts or Denver Brain Tumor Research Group 05 (DBTRG-05) MG cells by electroporation (*20*). DBTRG-05MG and U-87MG cells were from American Type Culture Collection (Rockville, MD). Cell spreading was assessed (*9*) 24 hours after transfection.
11. S. K. Akiyama, S. S. Yamada, W. T. Chen, K. M. Yamada, *J. Cell Biol.* **109**, 863 (1989).
12. Twenty-four hours after transfection GFP- or GFP-PTEN–expressing human foreskin fibroblasts or U-87MG cells were plated on cover slips coated with FN (10 μg/ml). Cells were allowed to spread for the indicated times (Fig. 3B) in Dulbecco's modified Eagle's medium (DMEM) containing 1% bovine serum albumin (BSA), fixed with 4% paraformaldehyde and 0.5% Triton X-100 in phosphate-buffered saline (PBS) for 5 min, and then incubated with 4% paraformaldehyde in PBS for an additional 20 min. Cytoskeletal proteins were visualized by incubating first with mouse mAbs to paxillin (0.5 μg/ml), tensin (5 μg/ml), FAK (5 μg/ml), or phosphotyrosine (10 μg/ml, PY20) from Transduction Laboratories (Lexington, KY), vinculin (VIN-11-5, 20 μg/ml, Sigma, St. Louis, MO), or rhodamine-labeled phalloidin (0.1 U/ml, Molecular Probes, Eugene, OR), and then with Cy-3–conjugated goat antibody to mouse immunoglobulin G (dilution 1/600, Jackson Immunoresearch Laboratories, West Grove, PA).
13. PTEN point mutants C124A ($Cys^{124} \rightarrow Ala$), D92A ($Asp^{92} \rightarrow Ala$), C124A/D92A (double mutant), and G129E ($Gly^{129} \rightarrow Glu$) were generated by site-directed mutagenesis through PCR and confirmed by DNA sequencing. U-87MG cells were transfected with 30 μg each of wild-type or mutant *PTEN* plasmids, or with hemagglutinin (HA)–tagged FAK with or without GFP or GFP-*PTEN*; alternatively, stable NIH 3T3 cell *PTEN* transfectants were induced for 5 days with 1 μM muristerone A. Cells were harvested with trypsin, resuspended for 45 min in DMEM containing 1% BSA, and then allowed to spread on dishes coated with FN (10 μg/ml). Cells were homogenized and analyzed for phosphotyrosine as described (*21*) with 4 to 20% SDS–polyacrylamide gradient gel electrophoresis (PAGE) (Novex, San Diego, CA).
14. C. O. Arregui, T. C. Leung, J. Balsamo, J. Lilien, *Mol. Biol. Cell* **8**, 290a (abstract) (1997).
15. E. A. Clark and J. S. Brugge, *Science* **268**, 233 (1995); J. T. Parsons, *Curr. Opin. Cell Biol.* **8**, 146 (1996); K. M. Yamada and B. Geiger, *ibid.* **9**, 76 (1997).
16. L. A. Cary, J. F. Chang, J.-L. Guan, *J. Cell Sci.* **109**, 1787 (1996); L. A. Cary, D. C. Han, T. R. Polte, S. K. Hanks, J.-L. Guan, *J. Cell Biol.* **140**, 211 (1998); R. L. Klemke *et al.*, *ibid.*, p. 961.
17. Histidine-tagged PTEN (His_6-PTEN) was generated by inserting full-length *PTEN* cDNA into the pQE30 vector (Qiagen, Valencia, CA). Expression of His_6-PTEN was induced by incubating transformed *E. coli* with 1 mM isopropyl β-D-galactopyranoside (IPTG) for 4 hours. The protein was purified with Ni-NTA (nitrilotriacetic acid) beads (Qiagen) under denaturing conditions and then renatured by sequential dilution and concentration in renaturation buffer [PBS (pH 7.0) containing 2 mM $MgCl_2$, 0.5 mM phenylmethanesulfonyl fluoride, 0.005% Tween-20, 10 mM dithiothreitol, and a protease inhibitor mixture (Boehringer Mannheim)]. Purity (>90%) was confirmed by SDS-PAGE and Coomassie blue staining. PTEN dephosphorylation of FAK was examined by an in-blot phosphatase assay: U-87MG cells that had spread on FN for 2 hours were lysed (*21*), and 10 μg of protein per lane was subjected to 4 to 20% SDS-PAGE and electrotransferred to nitrocellulose (*13*, *16*). Blots were incubated with recombinant His_6-PTEN (20 μg/ml) in 50 mM Hepes buffer (pH 7.0) containing 10 mM $MgCl_2$ and 10 mM dithiothreitol at 30°C for 1 hour (*3*). Control *E. coli* lysate was from GFP-*PTEN*–transformed cultures not induced by IPTG. Phosphoproteins were detected with anti-phosphotyrosine (*21*).
18. A. J. Flint, T. Tiganis, D. Barford, N. K. Tonks, *Proc. Natl. Acad. Sci. U.S.A.* **94**, 1680 (1997).
19. A. Richardson and J. T. Parsons, *Nature* **380**, 538 (1996).
20. S. E. LaFlamme, L. A. Thomas, S. S. Yamada, K. M. Yamada, *J. Cell Biol.* **126**, 1287 (1994).
21. M. O. De Nichilo and K. M. Yamada. *J. Biol. Chem.* **271**, 11016 (1996).

22. We thank K. Tanaka and T. Takino for helping perform double-blind spreading and cell morphology assays, B. Katz for valuable discussions, and S. Yamada for human foreskin fibroblasts.

2 February 1998; accepted 21 April 1998